

# Fitting Forms for Isothermal Data

Ralph Menikoff and Thomas D. Sewell

Theoretical Division

Los Alamos National Laboratory

Los Alamos, NM 87545

## Abstract

Isothermal data in the  $(V, P)$ -plane are generally not sufficiently precise to determine the bulk modulus and its pressure derivative using finite differences. Instead the data are fit to an analytic expression and the derivatives of the analytic expression are used. The derivatives obtained in this fashion may be sensitive to the fitting form and the domain of data used for the fit. This point is illustrated by re-analyzing two data sets for  $\beta$ -HMX. With the third order Birch-Murnaghan equation and a Hugoniot based fitting form we show that the uncertainty in the modulus due to the fitting forms is greater than the statistical uncertainty of the fits associated with the experimental error bars. Moreover, there is a systematic difference between the two data sets. Both fitting forms give statistically good fits for both experiments, although the modulus at ambient pressure ranges from 10.6 to 17.5 GPa. The large variation in the initial value of the modulus is due in part to the lack of data in the low pressure regime (below 1 GPa) and to the property of a molecular crystal, in contrast to a metal or atomic crystals, to stiffen substantially under a small amount of compression. The values of the modulus and its derivative are an important issue for an explosive like HMX because they affect predictions of the Hugoniot locus in the regime of the Chapman-Jouget detonation pressure.

# 1 Introduction

Hydrostatic compression experiments are used to measure the equilibrium pressure along an isotherm as a function of density. The isothermal bulk modulus and its derivative can then be computed. These quantities determine the Hugoniot locus for weak shocks in the form of a linear (shock velocity)-(particle velocity) relation. This technique can be applied to explosive crystals for which the inert Hugoniot is difficult to measure due to the reactive nature of the material.

The isothermal bulk modulus is defined by  $K_T = -V \frac{\partial P}{\partial V} |_T$  and its derivative by  $K'_T = \frac{dK_T}{dP} = -1 - V \frac{\partial^2 P}{\partial V^2} |_T / \frac{\partial P}{\partial V} |_T$ . Thermodynamic relations can be used to transform between isothermal and isentropic values:

$$K_S = \frac{K_T}{1 - (\beta T) \left( \frac{\beta V K_T}{C_P} \right)}, \quad (1)$$

$$K'_S = \frac{K'_T + (\beta T) \left( \frac{\beta V K_T}{C_P} \right)^2 + (\beta T) \left( \frac{\beta V K_T}{C_P} \right) \left[ \frac{\partial}{\partial \log T} \log K_T + \left( \frac{\beta V K_T}{C_P} \right) \frac{\partial}{\partial \log T} \log \left( \frac{\beta^2 V}{C_P} \right) \right]}{\left[ 1 - (\beta T) \left( \frac{\beta V K_T}{C_P} \right) \right]^2}, \quad (2)$$

where  $\beta$  is the coefficient of volumetric thermal expansion, and  $C_P$  is the specific heat at constant pressure. We note that  $\beta$  and  $C_P$  can be measured directly. Furthermore,

$$\frac{\beta V K_T}{C_P} = \frac{C_V}{C_P} \Gamma < \Gamma = O(1),$$

where  $\Gamma$  is the Grüneisen coefficient, and at ambient conditions  $\beta T \ll 1$ . Consequently, if as expected the temperature derivatives in equation (2) are on the order of 1 or less then their effect is small. Hence, we can neglect the temperature derivatives and obtain

$$K'_S \approx \frac{K'_T + (\beta T) \left( \frac{\beta V K_T}{C_P} \right)^2}{\left[ 1 - (\beta T) \left( \frac{\beta V K_T}{C_P} \right) \right]^2}. \quad (2')$$

For the principal Hugoniot locus, the intercept and slope of the  $u_s$ - $u_p$  relation are given by

$$c = \sqrt{K_S / \rho}, \quad (3)$$

$$s = (K'_S + 1) / 4, \quad (4)$$

where  $K_S$  and  $K'_S$  are evaluated at the initial state. These relations allow the Hugoniot to be determined from isothermal data over a limited domain of pressure, typically up to a shock pressure on the order of  $K_S$ . In general, the Grüneisen coefficient and specific heat are needed to extend a single isotherm  $P_T(V)$  to an equation of state  $P(V, e)$  needed to compute the Hugoniot locus.

The isothermal data are usually not sufficiently precise to be able to calculate derivatives by simple finite differences. Instead an analytic form for the isotherm  $P_T(V)$  is assumed. After fitting parameters to match the data, derivatives can be obtained analytically. In effect, the fitting form is used to smooth the data. An important question is the sensitivity of  $K_T$  and  $K'_T$  to the fitting form and to the domain of data used for the fit.

The choice of fitting form can have a large effect on the results of the data analysis. This point is illustrated by re-analyzing two data sets for  $\beta$ -HMX (monoclinic crystal of cyclo-tetramethylene-tetrinitramine) with the third order Birch-Murnaghan equation and a Hugoniot based fitting form. In this example, we show that the uncertainty in the modulus due to the fitting forms is greater than the statistical uncertainty of the fits associated with the experimental error bars. In spite of statistically good fits with both fitting forms for both experiments, the modulus at ambient pressure ranges from 10.6 to 17.5 GPa and the derivative of the modulus from 5.6 to 18.1. Though there is a systematic difference between the two data sets, this accounts for only part of the spread.

The large variations in the initial value of the modulus and its derivative are also due in part to the property of a molecular crystal, in contrast to a metal or atomic crystals, to stiffen substantially under a small amount of compression, together with the lack of data in the low pressure regime (below 1 GPa). This means that the initial values of the modulus and its derivative should be used with care. For example, linearizing the equation of state about the ambient state may not give a good approximation for the shock Hugoniot at pressures well below the bulk modulus. This is an important issue for an explosive like HMX because it affects predictions of the Hugoniot locus in the regime of the Chapman-Jouget (CJ) detonation pressure.

## 2 HMX data

Data on an isotherm of  $\beta$ -HMX were first reported by Olinger, Roof & Cady [1] in 1978. More recently the measurements were extended from 7.5 GPa to 42 GPa by Yoo & Cynn [2]. Though not specified we assume that both experi-

ments were performed at room temperature. The two experiments used the same general technique but were different in detail.

Olinger, Roof & Cady used a Bridgman anvil to compress a sample 0.2 mm thick and 0.3 mm in diameter. The sample consisted of small HMX crystals and NaF powder suspended in a methanol-ethanol mixture. The HMX density was determined by measuring the lattice parameters with X-ray diffraction. The pressure was deduced from the compression of NaF determined by X-ray diffraction. Yoo & Cynn used a diamond anvil to compress a sample 0.12 mm in diameter. Micron-sized HMX crystals were suspended in argon. Again, the HMX density was determined via X-ray diffraction. The pressure was determined via a ruby fluorescence technique. The data from both experiments were used to determine  $K_T$  and  $K'_T$ . However, a different fitting form was used in the analysis of each data set.

Olinger, Roof & Cady [1] used the Hugoniot relations,

$$\frac{V}{V_0} = 1 - \frac{u_p}{u_s},$$

$$P = P_0 + \rho_0 u_p u_s,$$

to transform each  $(V, P)$ -data point to a pseudo-particle velocity  $u_p$  and a pseudo-shock velocity  $u_s$ . The pseudo velocities can be expressed as

$$u_p = [(P - P_0)(V_0 - V)]^{1/2}, \quad (5)$$

$$u_s = V_0 \left[ \frac{P - P_0}{V_0 - V} \right]^{1/2}. \quad (6)$$

In the  $(u_p, u_s)$ -plane their data are well fit by a straight line,  $u_s = c_T + s_T u_p$ . This results in the fitting form

$$P(V) = \frac{V_0 - V}{[V_0 - s_T(V_0 - V)]^2} c_T^2. \quad (7)$$

From the fit they obtained  $K_{T0} = 13.5$  GPa and  $K'_{T0} = 9.3$ .

We note that for the Hugoniot locus of a solid, up to a pressure on the order of the bulk modulus compressional effects dominate thermal effects. Thus, within the experimental domain of pressure it is not surprising that a fitting form used for Hugoniot loci is a reasonable approximation to an isotherm.

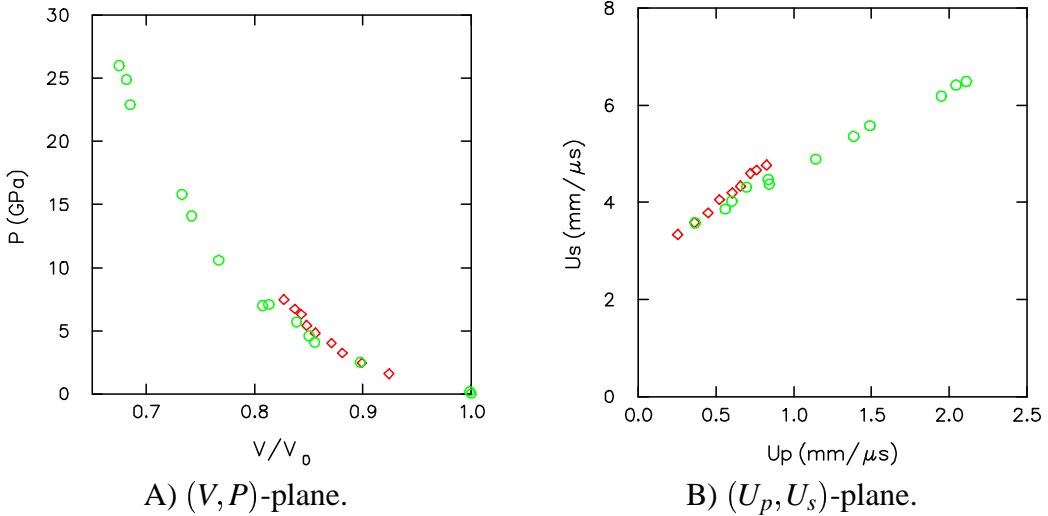


Figure 1: HMX isotherm data. Diamonds and circles are data from Olinger, Roof & Cady [1] and Yoo & Cynn [2], respectively.

Yoo & Cynn [2] fit their data to a third-order Birch-Murnaghan equation of state (see, *e.g.*, [3, p. 64])

$$P(V) = \frac{3}{2}K_{T0} \left[ \eta^{-7/3} - \eta^{-5/3} \right] \left[ 1 + \frac{3}{4}(K'_{T0} - 4)(\eta^{-2/3} - 1) \right], \quad (8)$$

where  $\eta = V/V_0$ . Their “best-fit” values are  $K_{T0} = 12.4$  GPa and  $K'_{T0} = 10.4$  for the data below a pressure of 27 GPa.

The reported results for the two experiments differ by 8.5% for the moduli and 11% for the derivative of the moduli. Both data sets are shown in Figure 1 in both the  $(V, P)$ -plane and the pseudo-velocity plane (Yoo & Cynn data below 27 GPa). Olinger, Roof & Cady listed the uncertainty in their data points. It is approximately 2% in pressure and varies from 0.1% to 1.5% in  $V/V_0$  as the compression ratio increases. Yoo & Cynn did not list the uncertainty explicitly but error bars were shown in the plots of [2, fig. 5]. From this we infer that their uncertainty in the pressure is about 0.1 GPa + 2% and their uncertainty in  $V/V_0$  is about 0.5%. It is natural to ask to what extent the difference in the bulk modulus inferred from the two data sets can be attributed to the different methods of analysis (*i.e.*, assumed fitting forms), to the uncertainty in the data points or to differences in the experiment (*i.e.*, crystal size, experimental geometry, pressure medium, and means of determining pressure).

This led us to reanalyze both data sets using both fitting forms. In the process

we found that a least square fit to the data reported by Yoo & Cynn, using their fitting form, leads to a value of  $K_{T0} = 14.7 \text{ GPa}$  which is 16% larger than what Yoo & Cynn quoted as their “best-fit”. However, this does not explain the discrepancy between the value of  $K_{T0}$  obtained from the two experiments. Nor is the difference within the uncertainty of the measurements.

### 3 Re-analysis of Data

The hydrostatic data of Yoo & Cynn [2] extend up to 42 GPa. In addition to measuring the pressure they measured the Raman spectra. There is evidence in the spectrum for phase transitions at 12 GPa and 27 GPa. At 12 GPa there is negligible volume change and they suggest the transition is martensitic. Since a crystal of  $\beta$ -HMX is anisotropic, hydrostatic compression gives rise to a shear strain which can induce a martensitic transition. At 27 GPa there is a 4% volume change. It is natural to limit the domain of the fits based on these transitions. Consequently, we have done two fits for Yoo & Cynn’s data. The domain of the data used for fitting does affect the values of the resultant parameters.

We note that both fitting forms have 2 parameters, and by construction both go through the initial state  $V/V_0 = 1$  and  $P = 0$ . The velocity parameters  $c_T$  and  $s_T$  in the  $(u_p, u_s)$ -plane and the Birch-Murnaghan parameters  $K_{T0}$  and  $K_{T0} \times K'_{T0}$  in the  $(V, P)$ -plane enter the fitting function as linear parameters. We determine these parameters from a least squares fit with weights specified by the uncertainty in the data points.

For the fit in the  $(V, P)$ -plane, we treated  $V$  as the independent variable and added the uncertainty in the measured value of  $V$  to the measured uncertainty in  $P$ :

$$(\delta P')^2 = (\delta P)^2 + \left( \frac{dP}{dV} \delta V \right)^2.$$

This results in a non-linear minimization problem for the fitting parameters. However, it can be solved by iterating on the linear problem. Only a few iterations are needed to obtain consistency between  $\delta P'$  and  $dP/dV$ .

For the fit in the  $(u_p, u_s)$ -plane we compute the uncertainties from eqs. (5) and (6) assuming that  $\delta V$  and  $\delta P$  are uncorrelated;

$$\left( \frac{\delta u_p}{u_p} \right)^2 = \left( \frac{\delta u_s}{u_s} \right)^2 = \frac{1}{2} \left( \frac{\delta P}{P} \right)^2 + \frac{1}{2} \left( \frac{\delta V}{V_0 - V} \right)^2.$$

With  $u_p$  as the independent variable the uncertainty in  $u_p$  is added to that of  $u_s$  in a

fitting form	$K_{T0}$ (GPa)	$K'_{T0}$	$\chi^2_v$	$c$ (km/s)	$s$
<b>Olinger, Roof &amp; Cady data set</b>					
pseudo-velocity	13.4	9.4	0.23	2.65	2.59
$\sigma$	$\pm 0.3$	$\pm 0.7$		$\pm 0.08$	$\pm 0.17$
Birch-Murnaghan	10.6	18.1	0.35	2.36	4.78
$\sigma$	$\pm 1.7$	$\pm 3.4$		$\pm 0.19$	$\pm 0.86$
<b>Yoo &amp; Cynn data set, <math>P &lt; 12</math> GPa</b>					
pseudo-velocity	17.2	5.7	0.84	3.01	1.68
$\sigma$	$\pm 0.5$	$\pm 0.7$		$\pm 0.14$	$\pm 0.18$
Birch-Murnaghan	16.0	7.3	0.70	2.90	2.07
$\sigma$	$\pm 2.5$	$\pm 1.4$		$\pm 0.22$	$\pm 0.36$
<b>Yoo &amp; Cynn data set, <math>P &lt; 27</math> GPa</b>					
pseudo-velocity	17.5	5.6	0.64	3.04	1.65
$\sigma$	$\pm 0.3$	$\pm 0.2$		$\pm 0.07$	$\pm 0.05$
Birch-Murnaghan	14.7	8.6	0.49	2.78	2.40
$\sigma$	$\pm 1.3$	$\pm 0.8$		$\pm 0.13$	$\pm 0.21$

Table 1: Results of fitting forms on the two data sets.

similar manner as described above for  $V$  and  $P$ . Again the fitting parameters were obtained by iterating the linear problem.

The least-squares fit to the data of Olinger, Roof & Cady is shown in Figure 2, and the least-squares fit to the data of Yoo & Cynn is shown in Figure 3. The values of the fitting parameters along with their standard deviations  $\sigma$  are listed in table 1. In addition, the value of the reduce chi-squared

$$\chi^2_v = \frac{1}{N-2} \sum_i \left( \frac{P_i - P(V_i)}{\delta P'} \right)^2 \quad (9)$$

is given for each case. In all cases,  $\chi^2_v < 1$ . Hence, the isothermal data can be fit equally well with both the Birch-Murnaghan and the Hugoniot functional form of  $P(V)$ .

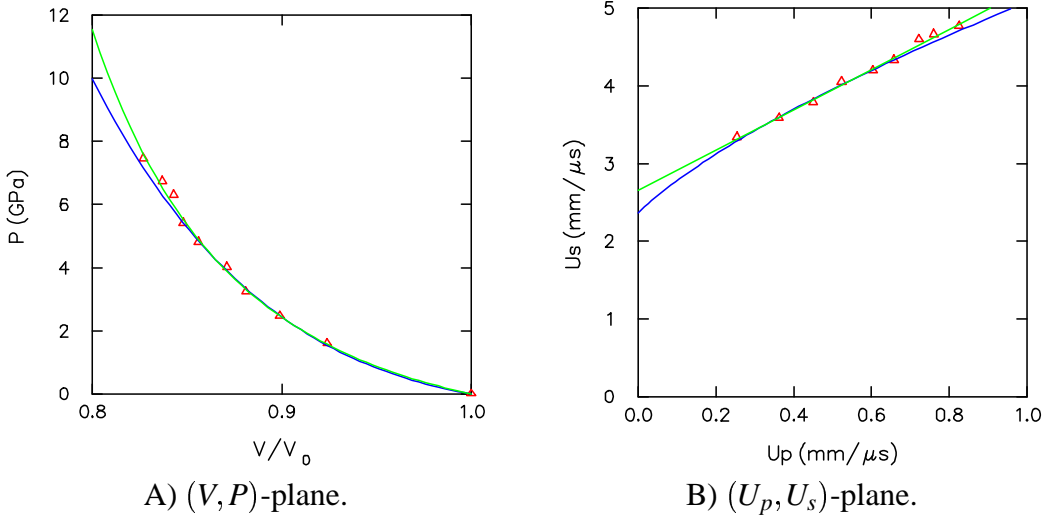


Figure 2: Fits to HMX data of Olinger, Roof & Cady [1]. Red symbols are data points. Green line is based on Hugoniot fitting form and blue line is based on Birch-Murnaghan fitting form.

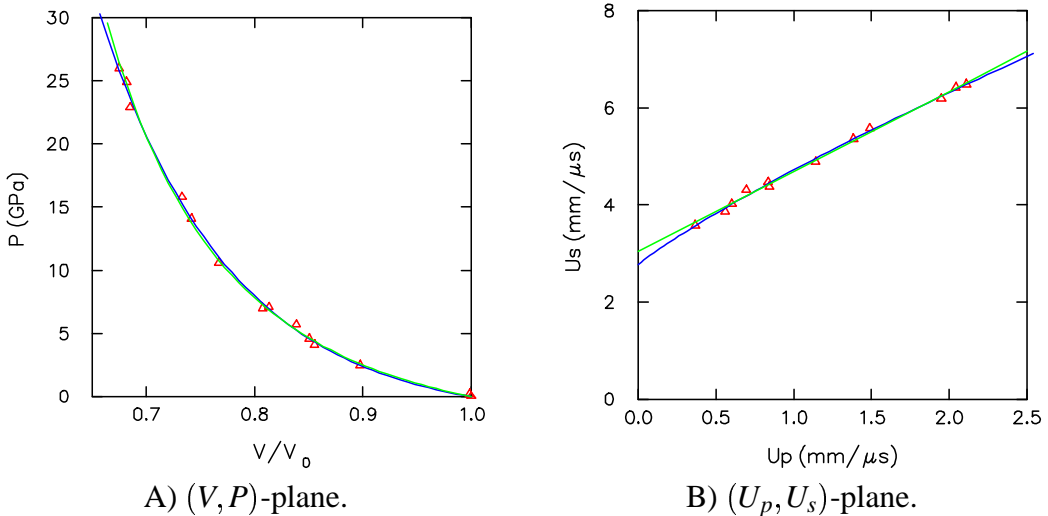


Figure 3: Fits to HMX data of Yoo & Cynn [2] (restricted to  $P < 27$  GPa). Red symbols are data points. Green line is based on Hugoniot fitting form and blue line is based on Birch-Murnaghan fitting form.

For the domain of the data,  $K \approx K_0 + PK'$ . In this approximation, the slope  $\frac{dP}{dV} = \frac{K_0}{V} \left(\frac{V_0}{V}\right)^{K'_0}$  and increases rapidly with increasing compression since  $K'_0$  is large. At high pressures the slope is large and the dominant contribution to  $\delta P'$  is from the uncertainty in  $V$ . This has a large effect on the value of  $\chi^2_v$  and the uncertainty in the fitting parameters. As an example of the magnitude of the effect, for the Birch-Murnaghan fit to the Yoo & Cynn data up to 27 GPa, setting  $\delta V = 0$  would increase  $\chi^2_v$  from 0.49 to 1.66. In addition, the uncertainties in the fitting parameters,  $\sigma_K$  and  $\sigma_{K'}$ , would decrease by about a factor of 2. Consequently, at high pressures it is important to measure  $V$  as accurately as possible.

A few observations about the fits, based on table 1, are instructive. For both the data of Olinger, Roof & Cady and the data of Yoo & Cynn in the pressure domain  $P < 27$  GPa, the differences in  $K_{T0}$  and  $K'_{T0}$  between the two fitting forms is greater than the sum of the statistical uncertainties in each fit due to the uncertainty in the data points. This is due to the curvature of  $u_s(u_p)$  for the Birch-Murnaghan fitting form when  $u_p$  is small. We discuss the curvature effect in more detail in the next section. The implication is that the assumed fitting form can be a dominant error in determining the modulus and its derivative at ambient conditions (1 atm).

Furthermore, for either fitting form, the difference in values of  $K_{T0}$  and  $K'_{T0}$  determined from the two data sets is greater than the statistical uncertainty in the fits. This is seen graphically in contour plots of  $\chi^2_v$  shown in figure 4 for the two fits to the two data sets. The largest contour is slightly larger but comparable to the statistical uncertainties in the parameters of the fit. The fact that the “error ellipses” don’t overlap implies there is a systematic difference between the experiments.

Yoo & Cynn [2] suggest that their pressure medium (argon) results in a more hydrostatic compression than the pressure medium (ethanol-methanol) used by Olinger, Roof & Cady [1]. Moreover, a non-hydrostatic compression would result in a larger volume for a given pressure [4] which is consistent with the difference between the data sets. However, it is not clear which medium is more hydrostatic. At room temperature argon solidifies at 1.3 GPa [5] whereas the ethanol-methanol mixture remains a liquid, albeit highly viscous, up to 10 GPa [6]. The fact that argon solidifies is mitigated by other properties. Argon is much softer (lower bulk modulus) and readily recrystallizes which tends to relieve the shear stress [7]. To some degree, both experiments are subject to a systematic error resulting from their pressure mediums not being perfectly hydrostatic at high pressures. Developing experimental techniques and methods of analysis to compensate for shear stress is an area of active research, see for example [4].

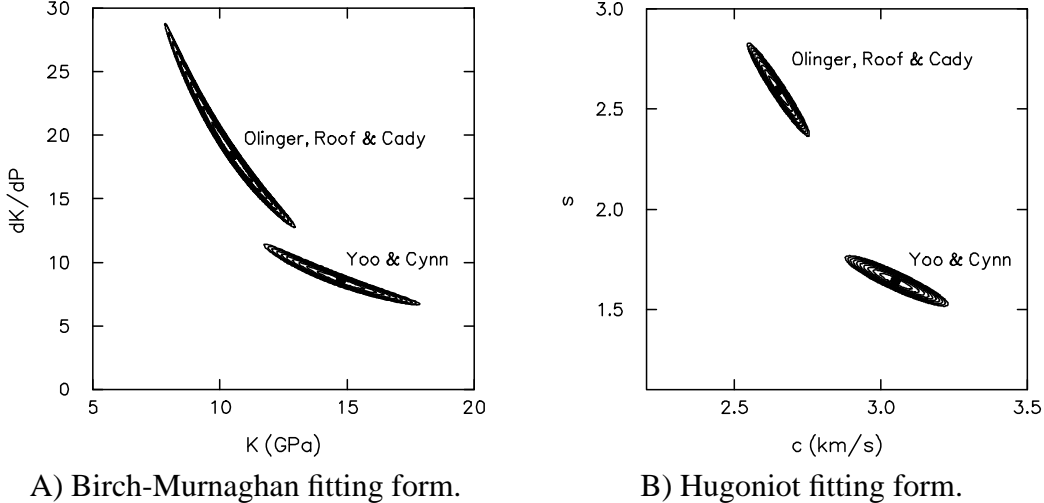


Figure 4: Contour plot of  $\chi^2_v$  for fits to the HMX data of Olinger, Roof & Cady [1] and Yoo & Cynn [2] (restricted to  $P < 27 \text{ GPa}$ ). Ten contour for each fit are equally spaced between the minimum value and twice the minimum of  $\chi^2_v$ .

Systematic differences between the two experiments may also result from the different methods for inferring the pressure and differences in experimental design such as the use of an axial versus radial x-ray beam to obtain the diffraction pattern from which the lattice parameters and hence the crystal density are inferred. In addition, during compression there is the possibility of a stick-slip effect giving rise to localized shear heating at the anvil surfaces or between grains, and thus causing a small amount of HMX to decompose. Until the discrepancy between the experiments is resolved fully the best one can say is that  $K_{T0} = 14 \pm 3.5 \text{ GPa}$  and  $K'_{T0} = 7.5 \pm 1.9$ . These are large uncertainties ( $\pm 25\%$ ) in important parameters.

The possibility of a martensitic phase transition at 12 GPa [2] suggests restricting the domain of data used for the fit. When the pressure domain of Yoo & Cynn's data is restricted from 27 to 12 GPa, the parameters  $c$  and  $s$  of the pseudo-velocity fit change by only 1%. In contrast the parameters  $K_{T0}$  and  $K'_{T0}$  of the Birch-Murnaghan fit change by 8% and 16%, respectively. These changes are within the error estimate. Considering that there is no volume change in the transition, the possible kink in the slope of  $P(V)$  at the phase transition is undoubtably lost in the scatter of the data. It is interesting to note that the parameters for the Hugoniot fitting form are less sensitive to the domain used for the fit than the parameters of the Birch-Murnaghan fit. This is due to the fact that there are no data points in the low pressure region in which the curvature of  $u_s(u_p)$  is greatest.

## 4 Discussion

A notable property of the Birch-Murnaghan fitting form is the curvature in the pseudo-velocity plane. As noted previously, for stiff materials such as solids, weak shocks are dominated by compressional effects and for low pressures the isotherm and the Hugoniot locus are expected to have a similar behavior. In contrast to metals, it is common for the Hugoniot loci of liquids [8], porous solids and polymers [9] to display significant curvature in the  $(u_p, u_s)$ -plane for weak shocks. The curvature effect also has been observed for the explosive PETN (PentaErythritol-TetraNitrate) [10] which is a large organic molecular crystal.

We think the mechanism in liquids and large molecular crystals is similar to what Olinger, Halleck & Cady [10] described for PETN. At low pressures, regions of relatively low intermolecular electron density are closed. This is analogous to squeezing out voids in porous solids and “free volume” in polymers. Further compression then requires distortion of intra-molecular degrees of freedom characterized by covalent bonding and/or accessing states successively higher on the intermolecular repulsive core. This leads to a large increase in the modulus over a relatively small pressure domain. The rapid increase in the modulus is the cause of the curvature of the Hugoniot loci in the velocity plane. It would not be surprising for HMX ( $C_4H_8N_8O_8$ ), which like PETN ( $C_5H_8N_4$ ) is a large organic molecular crystal, to display a similar curvature effect. In fact, Pastine and Bernicker [11] have analyzed TATB (TriAmino-Trinitro-Benzene,  $C_6H_6N_6O_6$ ) and have suggested that the hydrostatic equation of state of most secondary explosives would have a similar characteristic.

The strongest curvature effect usually occurs at pressures below a few kilobars. There is only one isothermal data point for HMX below 1.5 GPa. Consequently, to justify the use of the Birch-Murnaghan fitting form over the simpler Hugoniot fitting form would require additional low pressure data. Experimentally it is difficult to measure the density at low pressure with the precision necessary to determine accurately the moduli. An alternative is to determine the bulk moduli from sound speed measurements. Because of anisotropy of the crystal ( $\beta$ -HMX is monoclinic), it is necessary to determine the full elastic tensor. The isentropic modulus corresponds to the Reuss average bulk modulus, and eq. (1) then determines the isothermal modulus which can be compared with the fits to the hydrostatic data. Recently, Zaug [12] has partially determined the elastic tensor of HMX from sound speed measurements using the impulsive stimulated light scattering technique [13]. Pinning down  $K_{T0}$  in this way would greatly reduce the uncertainty in the fitting parameters.

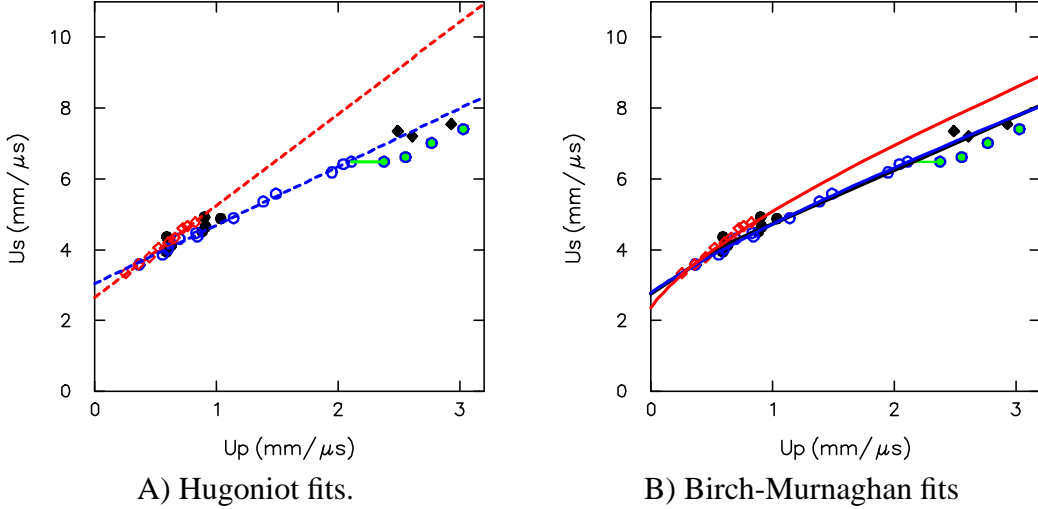


Figure 5: HMX data in  $(u_p, u_s)$ -plane. Red diamonds and blue circles are isothermal data of Olinger, Roof & Cady [1] and Yoo & Cynn [2], respectively. Black circles are Hugoniot data for solvent pressed HMX (0.5% porosity) [14, p. 596], and black diamonds are Craig's Hugoniot data for single crystal HMX (unspecified orientation) [15] and [14, p. 595] around the CJ-detonation pressure, 34–42 GPa. Green line indicates phase transition at 27 GPa in the isothermal data [2]. In addition: Dashed red and blue lines are linear fits to isothermal data. Black line is Bernecker's [17] proposed piecewise linear fit to Hugoniot data. Solid red and blue lines are Birch-Murnaghan fits to Olinger, Roof & Cady data and Yoo-Cynn data below phase transition at 27 GPa, respectively.

The uncertainty in  $K_{T0}$  and  $K'_{T0}$  has important implications for the HMX shock Hugoniot. Hydro simulations frequently use a Mie-Grüneisen equation of state for solids with a reference curve based on the principal Hugoniot and a linear  $u_s$ - $u_p$  relation for the Hugoniot locus, eq. (7). Both the isothermal data and the Hugoniot data for HMX are shown in figure 5. Extrapolating to CJ-detonation pressure,  $u_s \approx 9 \text{ mm}/\mu\text{s}$ , there is a large difference between the linear fits based on the data of Olinger, Roof & Cady and the data of Yoo & Cynn. Thus, the systematic difference between the two data sets has important consequences.

We note that there is also Hugoniot data for PBX-9501 [18], which is 95 wt% HMX. In the  $(u_p, u_s)$ -plane, the fit to the PBX-9501 Hugoniot data is closer to the fit to the data of Olinger, Roof & Cady than to the data of Yoo & Cynn. Moreover, recent measurements of the von Neumann spike of a detonation wave in PBX-9501 are compatible with extrapolating the low pressure Hugoniot data [19]. However, previous measurements in the HMX based PBX-9404 of Craig (reported

in [20, Table 1.4, p. 23]) obtained a von Neumann spike pressure compatible with the data of Yoo & Cynn. Finally, we note that there are three high pressure single crystal Hugoniot data points [15] and [14, p. 595]. Surprisingly, these data points imply that the single crystal is softer than the PBX.

Prior to Yoo & Cynn's recent experiment, Dick [16] and Bernecker [17] suggested a high pressure shock induced phase transition in HMX based on the fact that the high pressure Hugoniot data lay considerably below the straight line fit to the data of Olinger, Roof & Cady. This lead Bernecker [17] to propose approximating the Hugoniot locus with a piecewise linear fit. The Birch-Murnaghan fit to Yoo & Cynn's data below the phase transition at 27 GP is effectively a smooth version of Bernecker's fit. It interpolates between the low pressure data of Olinger, Roof & Cady (except for their 3 highest pressure data points) and the higher pressure data of Yoo & Cynn. Consequently, on the basis of the fit to Yoo & Cynn's data, a shock induced phase transition would not appear to be warranted.

Needless to say an accurate equation of state for HMX is a necessary ingredient for simulations used to determine initiation sensitivity. Understanding experimental errors and determining an equation of state consistent with all the data are important issues that require more attention.

## Acknowledgement

The authors wish to thank Drs. David Schiferl and Bart Olinger at LANL, and Dr. Choong-Shik Yoo at LLNL for explaining techniques and issues related to high pressure hydrostatic experiments.

## References

- [1] B. Olinger, B. Roof, and H. Cady. The linear and volume compression of  $\beta$ -HMX and RDX. In *Proc. Symposium (Intern.) on High Dynamic Pressures*, pages 3–8. C.E.A., Paris, France, 1978.
- [2] C.-S. Yoo and H. Cynn. Equation of state, phase transition, decomposition of  $\beta$ -HMX. *J. Chem. Phys.*, 111:10229–10235, 1999.
- [3] Jean-Paul Poirier. *Introduction to the Physics of the Earth's Interior*. Cambridge Univ. Press, Cambridge, UK, 1991.

- [4] A. K. Singh and C. Balasingh and H.-K. Mao and R. J. Hemley and J. Shu. *Analysis of lattice strains measured under nonhydrostatic pressure.* *J. Appl. Phys.*, 83:7567–7575, 1998.
- [5] F. Datchi, P. Loubeyre and R. LeToullec. *Extended and accurate determination of the melting curves of argon, helium, ice and hydrogen.* *Phys. Rev. B*, 61:6535–6546, 2000.
- [6] G. J. Piermarini, S. Block and J. D. Barnett. *Hydrostatic limits in liquids and solids to 100 kbar.* *J. Appl. Phys.*, 44:5377–5382, 1973.
- [7] L. W. Finger and R. M. Hazen and G. Zou and H. K. Mao and P. M. Bell. *Structure and compression of crystalline argon and neon at high pressure and room temperature.* *Appl. Phys. Lett.*, 39:892–894, 1981.
- [8] R. W. Woolfolk, M. Cowperthwaite, and R. Shaw. A “universal” Hugoniot for liquids. *Thermochimica Acta*, 5:409–414, 1973.
- [9] R. Menikoff and E. Kober. Equation of state and Hugoniot locus for porous materials:  $P$ – $\alpha$  model revisited. In *Shock Compression of Condensed Matter—1999*, eds. M. D. Furnish, L. C. Chhabildas, and R. S. Hixson, AIP, pages 129–132, 2000.
- [10] B. Olinger, P. M. Halleck, and H. H. Cady. *The isothermal linear and volume compression of PETN to 10 GPa and the calculated shock compression.* *J. Chem. Phys.*, 62:4480–4483, 1975.
- [11] D. J. Pastine and R. R. Bernecker.  *$P,V,E,T$  equation of state for 1,3,5-triamino-2,4,6-trinitrobenzene.* *J. Appl. Phys.*, 45:4458–4468, 1974.
- [12] J. M. Zaug. Elastic constants of  $\beta$ -HMX and tantalum, equation of state of supercritical fluids and fluid mixtures and thermal transport determinations. In *Proceedings of the Eleventh Detonation Symposium*, pages 498–509, 1998.
- [13] J. A. Rogers and M. Fuchs and M. J. Banet and J. B. Hanselman and R. Logan and K. A. Nelson. Optical system for rapid materials characterization with transient grating technique: Application to nondestructive evaluation of thin films used in microelectronics. *Appl. Phys. Lett.*, 71:225–227, 1997.

- [14] S. Marsh, editor. *LASL Shock Hugoniot Data*. Univ. Calif. press, 1980. On line, <http://lib-www.lanl.gov/books/shd.pdf>.
- [15] B. G. Craig. Data from shock initiation experiments. Technical report M-3-QR-74-1, Los Alamos Scientific Lab., 1974.
- [16] J. J. Dick. A comparison of the shock and static compression curves for four solid explosives. *Journal of Energetic Materials*, 1:275–286, 1983.
- [17] R. R. Bernecker. Observations on the Hugoniot for HMX. In *Shock Compression of Condensed Matter–1995*, eds. S. C. Schmidt, and W. C. Tao, AIP, pages 141–144, 1995.
- [18] J. J. Dick, A. R. Martinez, and R. S. Hixson. *Plane impact response of PBX-9501 and its components below 2GPa*. Technical report LA-13426-MS, Los Alamos National Lab., 1998.
- [19] R. L. Gustavsen, S. A. Sheffield, and R. R. Alcon. Progress in measuring detonation wave profiles in PBX-9501. In *Proceedings of the Eleventh Detonation Symposium*, pages 821–827, 1998.
- [20] C. L. Mader. *Numerical Modeling of Explosives and Propellants*, second edition. CRC Press, Boca Raton, Fl., 1998.